Bloch-point-mediated topological transformations of magnetic domain walls in cylindrical nanowires
Supplementary material

A. Wartelle,[1,*] B. Trapp,[2] M. Staňo,[3,†] C. Thirion,[3] S. Bochmann,[4] J. Bachmann,[4,5] M. Foerster,[6] L. Aballe,[6] T. O. Menteş,[7] A. Locatelli,[7] A. Sala,[7] L. Cagnon,[3] J.-C. Toussaint,[3] and O. Fruchart[8,‡]

[1]*Univ. Grenoble Alpes, CNRS, Grenoble INP[§], Institut Néel, F-38000 Grenoble, France*
[2]*Univ. Grenoble Alpes, CNRS, NEEL, F-38000 Grenoble, France*
[3]*Univ. Grenoble Alpes, CNRS, Institut Néel, F-38000 Grenoble, France*
[4]*Friedrich-Alexander Universität Erlangen-Nürnberg, Erlangen 91058, Germany*
[5]*Saint-Petersburg State University, Institute of Chemistry, Universitetskii pr. 26, 198504 St. Petersburg, Russia*
[6]*Alba Synchrotron Light Facility, CELLS, Barcelona, Spain*
[7]*Elettra-Sincrotrone Trieste, S.C.p.A., Trieste I-34012, Italy*
[8]*Univ. Grenoble Alpes, CNRS, CEA, Grenoble INP[¶], INAC-Spintec, F-38000 Grenoble, France*

(Dated: June 27, 2018)

I. XMCD-PEEM CONTRAST

In the main text we ascribe the various shadow XMCD-PEEM contrasts to either a BPW or a TVW. The former case is easy to identify owing to its axial symmetry, however the latter case is less intuitive[1]. Fig. S1 shows a simulation of the expected contrast for a TVW, based on the post-processing of the micromagnetic simulation of a DW at rest. While in all cases a breaking of symmetry in the contrast is expected compared with the BPW, the detail of the feature strongly depends on the DW azimuth[1] (see also Fig. S2b, steps 5 and 6).

Also, note that the width of the shadow contrast is much larger than the wire diameter, which stems from low angle of incidence of the X-ray beam on the sample. To set numbers, the latter is $16°$, which translates into a lateral expansion of the shadow by a ratio 3.6. Thus, the scale bars indicates the true distance along the wire axis, whereas all lengths in the shadow are inflated along the beam direction.

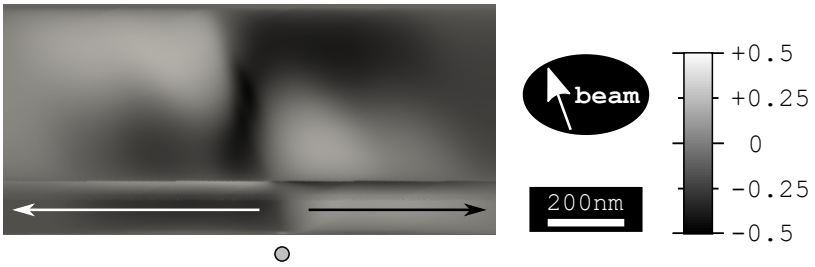

Fig. S1: Simulated XMCD-PEEM contrast for a tail-to-tail TVW in a permalloy nanowire with a diameter of 140 nm, with a beam in-plane angle of $70\,^\circ$ with respect to the wire axis. The center of the wall is indicated by a small disk outside below the wire. The shadow area does display an isolated bright area within the zone of dark contrast (to the right side of the wall here), in agreement with the experiment imaging (e.g. Fig. 2d of the main text).

[§] Institute of Engineering Univ. Grenoble Alpes
[¶] Institute of Engineering Univ. Grenoble Alpes
*Electronic address: alexis.wartelle@neel.cnrs.fr
†Present address: CEITEC - Central European Institute of Technology, Brno University of Technology, 612 00 Brno, Czech Republic
‡Electronic address: olivier.fruchart@cea.fr

II. SERIES OF DW TRANSFORMATIONS

Fig. S2 shows two sequences of field-induced DW motion performed at the same location in the same wire, first with a tail-to-tail domain state, then with a head-to-head domain state. Steps 2-7 in (a) is the same data as in Fig.1 of the main text. These series illustrate several aspects:

- The DWs stop at two well-defined locations in this wire. While the origin of pinning in such wires is difficult to correlate with structural defects even with the combined use of magnetic and structural imaging in a transmission electron microscopy[2], the distribution of pinning fields is broad and may range from well below 1 mT to $10 - 20$ mT, along the same wire and also depending on the material and wire diameter[3]. In the present case the distance of motion is approximately 2 µm, which is expected to be more than enough to allow the transformation to occur [see the indicator $z(t)$ in Fig.4 of the main text].
- The data illustrates the claim of the main text that DWs may change their topology only above a threshold of field, around 15 mT for the TVW-to-BPW transformation, and 20 mT for the reverse process.
- Transformations seem deterministic, see the comparison of both columns for the first five steps, which are perfectly mirroring each other.
- A TVW may display different azimuths (Fig. S2b, steps 5 and 6). This case also illustrates that a DW may change its feature (here, simply the azimuth, not the topology) without a net displacement over the full precessional dynamics during the pulse of field.

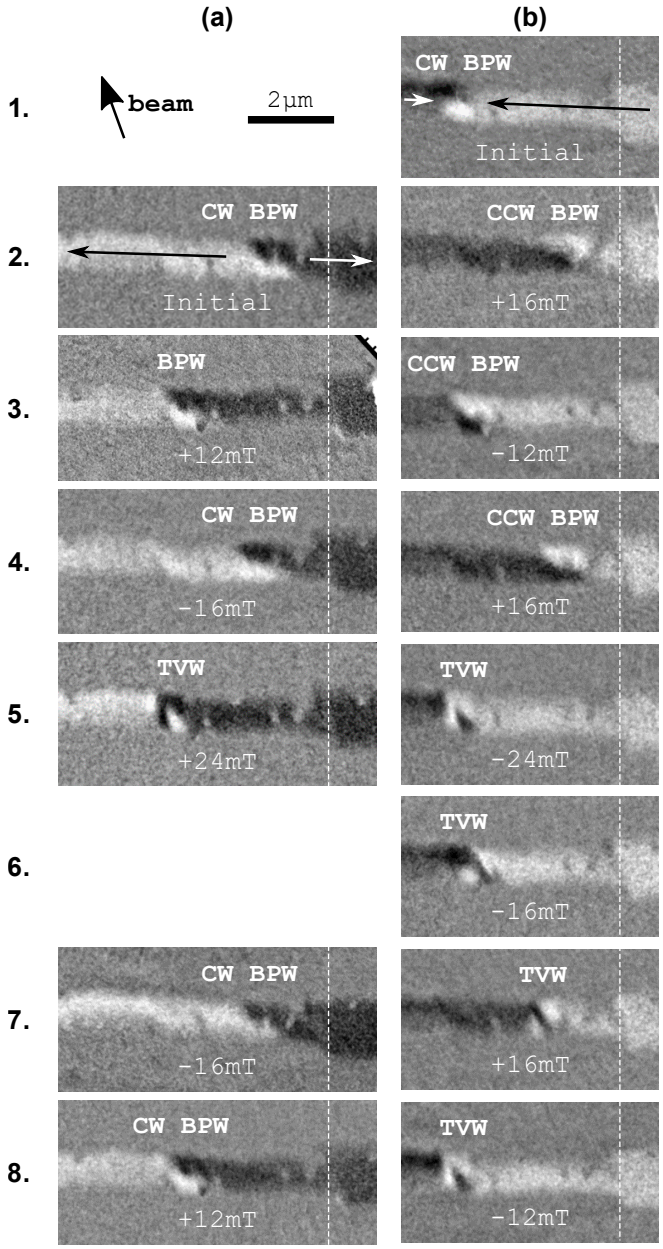

Fig. S2: Two eight-step sequences of back-and-forth field-induced DW motion between two pinning sites in a 140 nm-diameter $Fe_{20}Ni_{80}$ nanowire, with first a (a) tail-to-tail, and later a (b) head-to-head domain state. In these images, contrast is seen only in the shadow, due to the choice of microscope focus. Two extra steps were followed in the latter case. Arrows stand for magnetization in the domains, and the vertical dotted line indicates a diameter modulation. The circulation of the BPW is mentioned, either clockwise (CW) or counter-clockwise (CCW).

III. CONI ALLOYS

Fig. S3 provides an example of the experimental transformation of DW topology in a $Co_{40}Ni_{60}$ nanowire, instead of $Fe_{20}Ni_{80}$ nanowire in the main text. Here, starting from a TVW, the end state is a BPW. This shows that the effect evidenced does not depend on a specific sample or material.

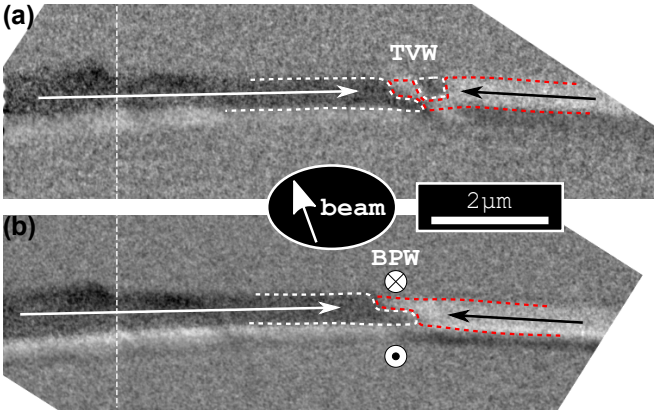

Fig. S3: Shadow XMCD-PEEM views of a $Co_{40}Ni_{60}$ nanowire before (a) and after (b) application of a -9 mT DC magnetic field approximately aligned with the structure axis. Arrows stand for magnetization in the domains, and the vertical dotted line indicates the diameter modulation. The X-Ray beam direction is indicated, along with the scale bar. The settings of focus are such that the wire surface is clearly visible (on the front size of the shadow, with respect to the incoming beam), with domains of contrast opposite to the in the shadow, as expected. The white (resp. red) dashed lines delimit the areas of opposite shadow contrast, highlighting the distinct DW patterns[4].

IV. PARAMETRIC MODEL

The parametric model displayed in Fig. 3a-b in the main text is built with a mathematical function chosen to yield topological features similar to those of the vector map of magnetization at the surface of the wire. However, the function does not have a specific meaning, and other choices may have been made. We start from the polynomial function $P(x, y, t) = -y^3 + x^2 + ty + 1$, rotated by $3\pi/4$. t is the parameter allowing to map various cases. The map mimicking magnetization is obtained by the normed vectors perpendicular to the gradient of $P(x, y, t)$, thus with local direction: $(-\mathrm{d}P/\mathrm{d}y, \mathrm{d}P/\mathrm{d}x)$. The maps in Fig. 3a-b in the main text are obtained for $t = -5$ and $t = 2$, respectively, so that the pseudo-time mentioned in the main text is defined as: $\tau = (t + 5)/7$. Finally, to avoid graphical artifacts associated with the singularities of hyperbolic and elliptical points, we lift the latter while leaving mostly unaffected the vector field, by renormalizing the set of coordinates with $(x, y)/\sqrt{(\epsilon + x^2 + y^2)}$. In practice we use $\epsilon = 0.01$.

V. VIDEOS

Two videos of surface magnetization illustrate the propagation of the TVW below and above the threshold field, for a permalloy wire of diameter 70 nm. One is under applied field 6 mT and lasts 9.2 ns, while the other is under 8.2 mT and lasts 0.64 ns.

[1] S. Jamet, S. D. Col, N. Rougemaille, A. Wartelle, A. Locatelli, T. O. Mente s, B. S. Burgos, R.Afid, L. Cagnon, J. Bachmann, S. Bochmann, O. Fruchart, , and J. C. Toussaint, Phys. Rev. B **92**, 144428 (2015).

[2] O. Fruchart *et al.*, unpublished.

[3] S. Da Col, S. Jamet, M. Staňo, B. Trapp, S. L. Denmat, L. Cagnon, J. C. Toussaint, and O. Fruchart, Appl. Phys. Lett. **109**, 062406 (2016), URL http://dx.doi.org/10.1063/1.4961058.

[4] S. Da Col, S. Jamet, N. Rougemaille, A. Locatelli, T. O. Mentes, B. S. Burgos, R. Afid, M. Darques, L. Cagnon, J. C. Toussaint, and O. Fruchart, Phys. Rev. B **89**, 180405 (2014).